Towards developed hydrodynamic turbulence

E.A. Kuznetsov

Lebedev Physical Institute, Moscow, Russia

Landau Institute for Theoretical Physics, Moscow, Russia

Novosibirsk State University, Novosibirsk, Russia

VII-th INTERNATIONAL CONFERENCE ”SCT-17”

Chernogolovka, Landau Institute, May 21-25, 2017

Joined with:

D.S. Agafontsev (Shirshov Institute & NSU),

A.A. Mailybaev (IMPA, Brazil)

OUTLINE

- Motivation: Collapse and the Kolmogorov-Obukhov theory
- Vortex line representation (VLR)
- Compressibility of VLR and folding of vortex lines
- Numerical experiment

Motivation: Collapse and the Kolmogorov-Obukhov theory

- According to the Kolmogorov-Obukhov theory (1941) velocity fluctuations at spatial scales l from the inertial range obey the power-law $\langle|\delta v|\rangle \propto \varepsilon^{1/3} l^{1/3}$, where ε is the mean energy flux from large to small scales. This formula is easily obtained from the dimensional analysis.
- Similarly, fluctuations for the vorticity field $\omega = \nabla \times \mathbf{v}$ diverge at small scales as $\langle|\delta\omega|\rangle \propto \varepsilon^{1/3} l^{-2/3}$, while the time of energy transfer from the energy-contained scale l_E to the viscous ones is finite and estimated as $T \sim l_E^{2/3} \varepsilon^{-1/3}$.
- These two relations allow to link the Kolmogorov spectrum formation with the blowup in the vorticity field (collapse).

Motivation: Collapse and the Kolmogorov-Obukhov theory

- Kolmogorov's arguments assume locality of interaction and isotropy of the turbulence in the inertial interval. This implies that the dynamics at these scales can be described by the Euler equations and the emergence of the Kolmogorov energy spectrum can be expected before the viscous scales are excited, i.e., in a fully inviscid flow.
- This conjecture was verified numerically in our previous papers (2015, 2016, 2017), where we showed that the Kolmogorov spectrum is developed through the formation of pancake-like structures of enhanced vorticity. Such pancakes can be treated as coherent structures.
- At the stage of turbulence onset turbulenceis far from isotropic, its spectrum contains a few number of jets. Each jet corresponds to its own pancake.

Motivation: Collapse and the Kolmogorov-Obukhov theory

- We also established numerically the asymptotic Kolmogorov-type scaling,

$$\omega_{\max}(t) \propto \ell(t)^{-2/3},$$

between the vorticity maximum on the pancake and the pancake thickness.

- No tendency to finite-time blowup was observed for generic initial conditions, with nearly exponential growth of vorticity in time.
- In the present paper we develop a new concept of folding for continuously distributed vortex lines.

Motivation: Collapse and the Kolmogorov-Obukhov theory

- The underlying idea that enables the folding phenomenon is that the "flow" of continuously distributed vortex lines is compressible, despite the incompressibility of the fluid: the vortex lines representation (VLR), E.K.& V. Ruban, 1998. Our new theory based on the VLR explains the $2/3$-law as a result of the classical fold catastrophe.
- The discussed approach is applicable for a larger class of "frozen-in-fluid" fields advected by incompressible fluid, for instance, the magnetic field in MHD or the di-vorticity field for 2D Euler.
- By means of a new adaptive numerical scheme based on the VLR we observed numerically the compressible character of continuously distributed vortex lines and verified the details of the folding phenomenon.

Vortex line representation (VLR)

Consider a frozen-in-fluid divergence-free field $\mathbf{B}$, defined from the following equation:

$$\frac{\partial \mathbf{B}}{\partial t} = \mathrm{rot}(\mathbf{v} \times \mathbf{B}), \ \mathrm{div}\, \mathbf{v} = 0.$$

Examples of such fields are the vorticity $\omega = \nabla \times \mathbf{v}$ for the 3D Euler equations, the magnetic field in (ideal) MHD and the divorticity field $\mathbf{B} = \nabla \times \omega$ for 2D Euler hydrodynamics. Such a $\mathbf{B}$-field line can only be changed by the velocity component $\mathbf{v}_n$ perpendicular to $\mathbf{B}$. Now we introduce a new type of trajectories given by the normal velocity component as

$$\frac{d\mathbf{x}}{dt} = \mathbf{v}_n(\mathbf{x}, t), \ \ \mathbf{x}|_{t=0} = \mathbf{a}.$$

Vortex line representation (VLR)

Because of frozenness of the field $\mathbf{B}$ a solution $\mathbf{x} = \mathbf{x}(\mathbf{a}, t)$ describes the motion of field lines. In terms of this mapping, Eq. for $\mathbf{B}$ admits explicit integration

$$\mathbf{B}(\mathbf{x}, t) = \frac{\widehat{J}\,\mathbf{B}_0(\mathbf{a})}{J}, \quad \widehat{J}(\mathbf{a}, t) = \left[\frac{\partial x_i}{\partial a_j}\right], \quad J = \det \widehat{J},$$

where $\mathbf{B}_0(\mathbf{a})$ is the initial field at $t = 0$ (analogous to the Cauchy invariant) and $\widehat{J}$ is the Jacobi matrix of the mapping. The inverse of the Jacobian, $n = 1/J$, has the meaning of a density which satisfies the continuity equation

$$\frac{\partial n}{\partial t} + \mathrm{div}(n\mathbf{v}_n) = 0.$$

Vortex line representation (VLR)

In case of the 3D hydrodynamics, Eqs. written for the vorticity $\mathbf{B} = \omega$ together with the relation $\omega = \nabla \times \mathbf{v}$ are called the vortex lines representation (VLR), and form a complete set of equations equivalent to the Euler equations. However, these equations are written in mixed Eulerian ($\mathbf{x}$-space) and Lagrangian ($\mathbf{a}$-space) variables. For numerical study, we now rewrite all the equations using the Eulerian variables.
Let $\mathbf{a} = \mathbf{a}(\mathbf{x}, t)$ be the inverse mapping. This mapping obeys the equation

$$\frac{\partial \mathbf{a}}{\partial t} + (\mathbf{v}_n \cdot \nabla)\mathbf{a} = 0.$$

Vortex line representation (VLR)

Eq. for the vorticity $\mathbf{B} = \omega$ can be rewritten in the form

$$\omega_i(\mathbf{x}, t) = \frac{1}{2}\varepsilon_{ijk}\,\varepsilon_{\alpha\beta\gamma}\,\omega_{0\alpha}(\mathbf{a})\,\frac{\partial a_\beta}{\partial x_j}\,\frac{\partial a_\gamma}{\partial x_k}.$$

Here $\omega_0(\mathbf{a})$ is the initial vorticity at $t = 0$. The two equations together with the relations

$$\mathbf{v} = \mathrm{rot}^{-1}\omega = -\Delta^{-1}\,(\nabla \times \omega), \quad \mathbf{v}_n = \mathbf{v} - \frac{(\mathbf{v}\cdot\omega)}{\omega^2}\omega$$

for the velocity and the normal velocity represent complete VLR system of equations written in the Eulerian coordinates $(\mathbf{x}, t)$.

Folding of vortex lines

REMARK 1: Wave breaking, as blowup, is well known for compressible flows resulting in appearance of shocks, which can be considered as the formation of folds. Breaking in gasdynamics is possible due to compressible character of the mapping.

REMARK 2: Breaking/folding of vortex lines is impossible in 2D and for cylindrically symmetric flows without swirl (Majda, 1990) because $\omega \perp \mathbf{v}$ and $\operatorname{div} \mathbf{v}_n = 0$, and consequently $J = 1$.

Thus, breaking/folding of vortex lines is 3D phenomenon.

Up to now it has not been known whether this process happens in a finite or infinite time.

Folding of vortex lines

In our numerics exponential increasing of the vorticity maximum and formation around this maximum a structure of the pancake type with exponential decreasing of its width wereobserved, instead of blow-up. Such structures appear around each vorticity maximum and are shown to have self-similar behavior. (First numerics by M. Brachet, et. el. (1992).)

Geometrically breaking results in touching of vortex lines (in a finite or infinite time).

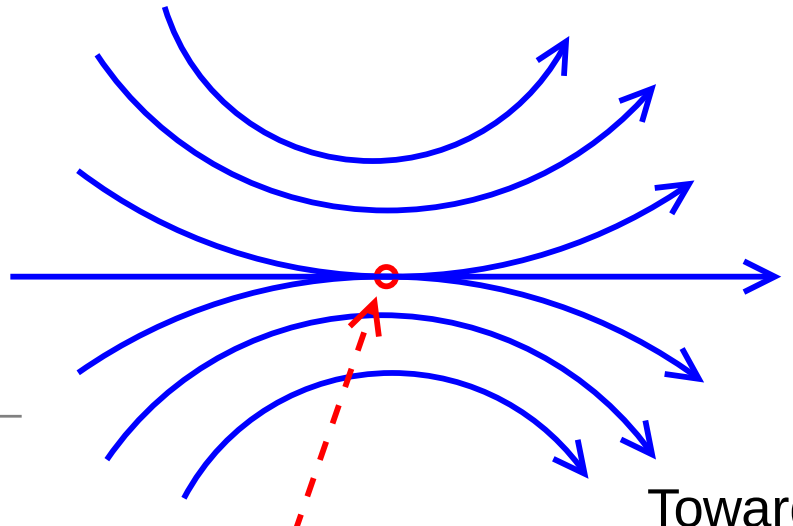

Folding of vortex lines

Let us assume that breaking/folding takes place. Consider the equation $J(\mathbf{a},t)=0$ and find its positive roots $t=\tilde{t}(\mathbf{a})>0$. Then the collapse (or touching) time will be

$$t_0=\min_a \tilde{t}(\mathbf{a}).$$

Near the minimal point $\mathbf{a}=\mathbf{a}_0$ as the expansion of J takes the form:

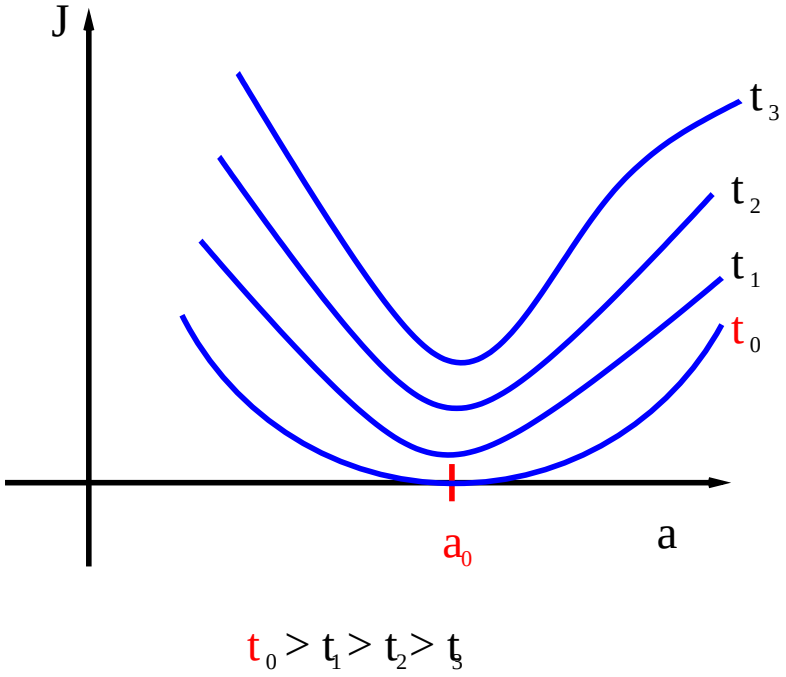

$$J(a,t)=\alpha\tau(t)+\gamma_{ij}\Delta a_i\Delta a_j$$

- concavity condition

$\alpha>0$, $\tau(t)\to 0$ as $t\to t_0$,

γ_{ij} is positive definite (non-degenerate) time independent matrix,

$\Delta\mathbf{a}=\mathbf{a}-\mathbf{a}_0$.

Self-similar asymptotics

REMARK: The assumption about linear dependence of J_{min} on $\tau(t)$ is familiar to the Landau assumption in his theory of the second-order phase transitions.
This expansion results in the self-similar asymptotics for vorticity:

$$\omega(\mathbf{r},t) = \frac{(\omega_{\mathbf{0}}(\mathbf{a})\cdot\nabla_a)\mathbf{r}|_{a_0}}{\tau(\alpha+\gamma_{ij}\eta_i\eta_j)}, \quad \eta = \frac{\Delta a}{\tau^{1/2}}.$$

Now the main problem is
to transform from the auxiliary a-space to the physical $\mathbf{r}$-space.

Self-similar asymptotics

Consider first the 1D case when

$$J = \frac{\partial x}{\partial a} = \alpha\tau + \gamma a^2 \quad \rightarrow x = \alpha\tau a + \frac{1}{3}\gamma a^3.$$

Thus, $a \sim \tau^{1/2}, \;\; x \sim \tau^{3/2}$, i.e. in the physical space compression happens more rapidly than in the space of Lagrangian markers !! At distances $\gamma a^2 \gg \alpha\tau$ we have the time-independent asymptotics,

$$J \sim x^{2/3}.$$

Thus, any changes happen at the region $\gamma a^2 \leq \alpha\tau$.

Self-similar asymptotics

3D case

The Jacobian $J = \lambda_1\lambda_2\lambda_3 \to 0$ means that one eigenvalue, say, $\lambda_1 \to 0$ and $\lambda_2, \lambda_3 \to$ const as $t \to t_0$ and $a \to a_0$. Hence it follows that near singular point there are two different self similarities:

along "soft" (λ_1) direction $x_1 \sim \tau^{3/2}$ (like in 1D);

along "hard" (λ_2, λ_3) directions $x_{2,3} \sim \tau^{1/2}$,

so that

$$\omega = \frac{1}{\tau}\mathbf{g}\left(\frac{x_1}{\tau^{3/2}}, \frac{x_\perp}{\tau^{1/2}}\right).$$

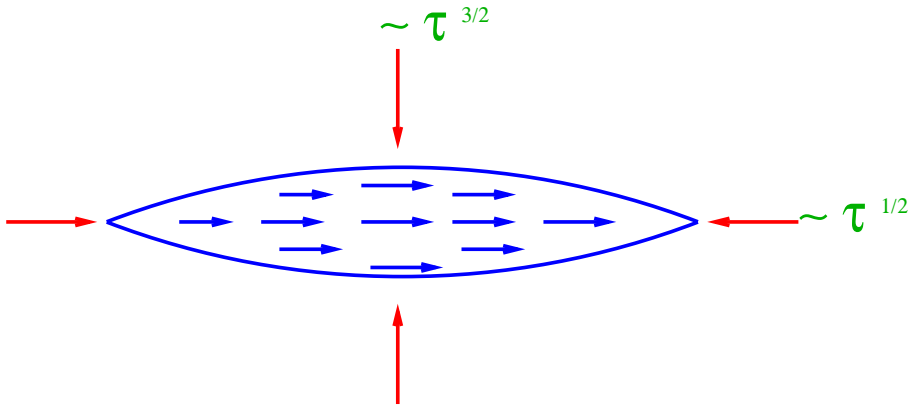

This results in formation

of pancake structure

(compare with Zeldovich)

Self-similar asymptotics

As $\tau \to 0$ when $\gamma_{ij}\Delta a_i \Delta a_j \gg \alpha\tau$ the vorticity has a time-independent, very anisotropic distribution. The main dependence of ω is connected with x_1-direction:

$$\omega \approx \frac{\mathbf{b}}{x_1^{2/3}}$$

with $\mathbf{b} = \text{const}$ and KOLMOGOROV index $2/3$!.
This dependence is realized everywhere except regions between two cubic paraboloids $-cx_\perp^3 < x_1 < cx_\perp^3$ In this narrow region vorticity at $\tau = 0$ behaves like

$$\omega \approx \frac{\mathbf{b_1}}{x_\perp^2}.$$

Self-similar asymptotics

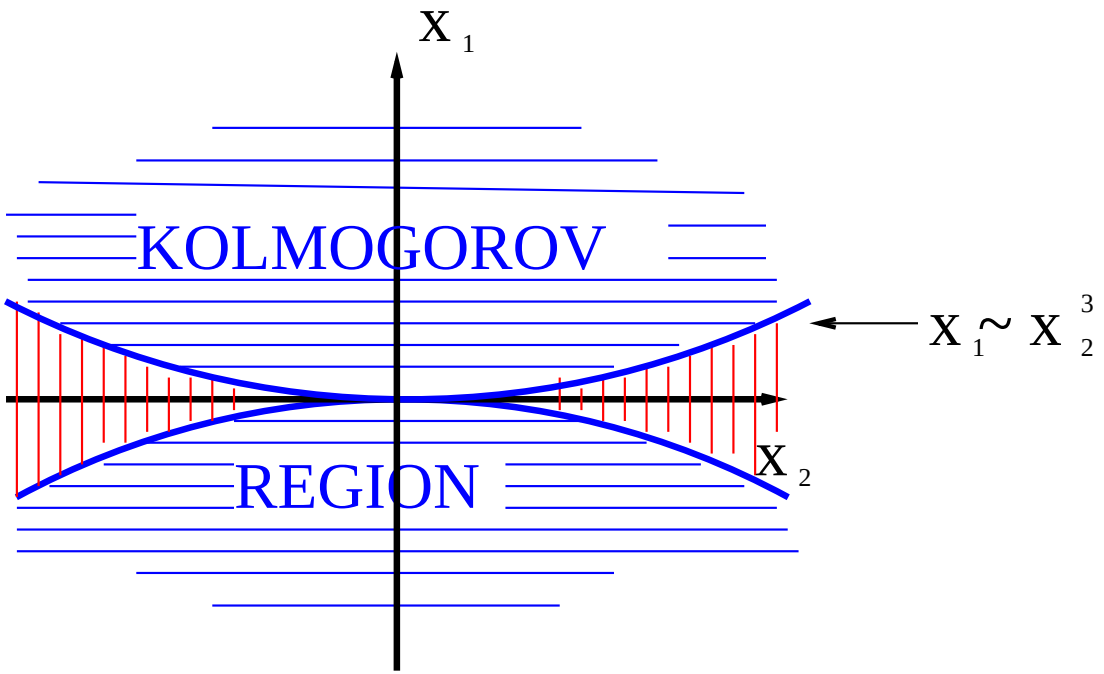

In Kolmogorov region the vorticity can be estimated as

$$\omega \sim \frac{P^{1/3}}{x_1^{2/3}}$$

where $P \sim \omega_0^3 L^2,\ L \sim \gamma^{-1/2}$.

VLR for exact solution

As it was reported by D. Agafontsev 3D Euler has exact solution which in Cartesian coordinates has the form

$$\mathbf{v}(\mathbf{x},t) = -\omega_{\max}(t)\,\ell_1(t)\,f\left(\frac{x_1}{\ell_1(t)}\right)\mathbf{n}_3 + \begin{pmatrix} -\beta_1(t)\,x_1 \\ \beta_2(t)\,x_2 \\ \beta_3(t)\,x_3 \end{pmatrix},$$

$$\omega(\mathbf{x},t) = \omega_{\max}(t) f'\left(\frac{x_1}{\ell_1(t)}\right)\mathbf{n}_2.$$

Here $\omega_{\max}(t)$ and $\ell_1(t)$ are the vorticity maximum and the pancake thickness, $f(x_1)$ is arbitrary smooth function.

VLR for exact solution

$\beta_1(t)$, $\beta_2(t)$ and $\beta_3(t)$ are given by

$$\beta_1 = -\dot{\ell}_1/\ell_1, \quad \beta_2 = \dot{\omega}_{\max}/\omega_{\max}, \quad -\beta_1 + \beta_2 + \beta_3 = 0.$$

Comparison of this solution with the simulations gives a good agreement at the pancake region for $\omega_{\max}(t) \propto e^{t/T_\omega}$ and $\ell_1(t) \propto e^{-t/T_\ell}$.

The velocity component normal to vorticity:

$$\mathbf{v}_n(\mathbf{x},t) = -\omega_{\max}(t)\,\ell_1(t)\,f\left(\frac{x_1}{\ell_1(t)}\right)\mathbf{n}_3 + \begin{pmatrix} -\beta_1 x_1 \\ 0 \\ \beta_3 x_3 \end{pmatrix}.$$

VLR for exact solution

For exponential pancake development the VLR mapping is written as

$$x_1 = a_1\, e^{-\beta_1 t}, \quad x_2 = a_2, \quad x_3 = a_3\, e^{\beta_3 t} - f(a_1)\, \frac{\sinh(\beta_3 t)}{\beta_3},$$

with the corresponding Jacobi matrix,

$$\hat{J}(\mathbf{a}, t) = \left[\frac{\partial x_i}{\partial a_j}\right] = \begin{pmatrix} e^{-\beta_1 t} & 0 & 0 \\ 0 & 1 & 0 \\ -f'(a_1)\, \frac{\sinh(\beta_3 t)}{\beta_3} & 0 & e^{\beta_3 t} \end{pmatrix}, \quad J(\mathbf{a}, t) = \det \hat{J} = e^{-\beta_2 t}.$$

VLR for exact solution

Respectively, for vorticity we have

$$\omega(\mathbf{x},t) = \frac{\widehat{J}\,\omega_0(\mathbf{a})}{J},$$

that coincides with our solution.

Hence the Jacobian is inverse-proportional to the vorticity $J(t) \propto 1/\omega_{\max}(t)$, and does not depend on spatial coordinates.

Numerical experiment

We use two numerical schemes based on direct integration of the Euler equations for ω and in the VLR formulation in the periodic box $\mathbf{r} = (x, y, z) \in [-\pi, \pi]^3$ using the pseudo-spectral method with high-order Fourier filtering. During simulations, the number of nodes is adapted independently along each coordinate providing an optimal anisotropic rectangular grid. We tested several large-scale initial conditions in the form of random truncated (up to second harmonics) Fourier series considered as a perturbation of the shear flow $\omega_x = \sin z,\ \omega_y = \cos z,\ \omega_z = 0$. This paper is based on one selected simulation with the final grid $486 \times 1024 \times 2048$.

Numerical experiment

- By means of the VLR scheme it was demonstrated decreasing of the Jacobian. This means that formation of the pancake structures can be considered as folding (breaking) of the vorticity lines.
- By use of the direct integration we found that at the maximal vorticity point

$$\frac{1}{\omega_{max}}\frac{d\omega_{max}}{dt} \simeq -\mathrm{div}\,\mathbf{v_n}.$$

This means that the main contribution into the vorticity maximum comes from the denominator,

$$\omega(\mathbf{r},t) = \frac{(\omega_0(\mathbf{a})\cdot\nabla_a)\mathbf{r}(\mathbf{a},t)}{J(\mathbf{a},t)}.$$

Numerical experiment: compressibility

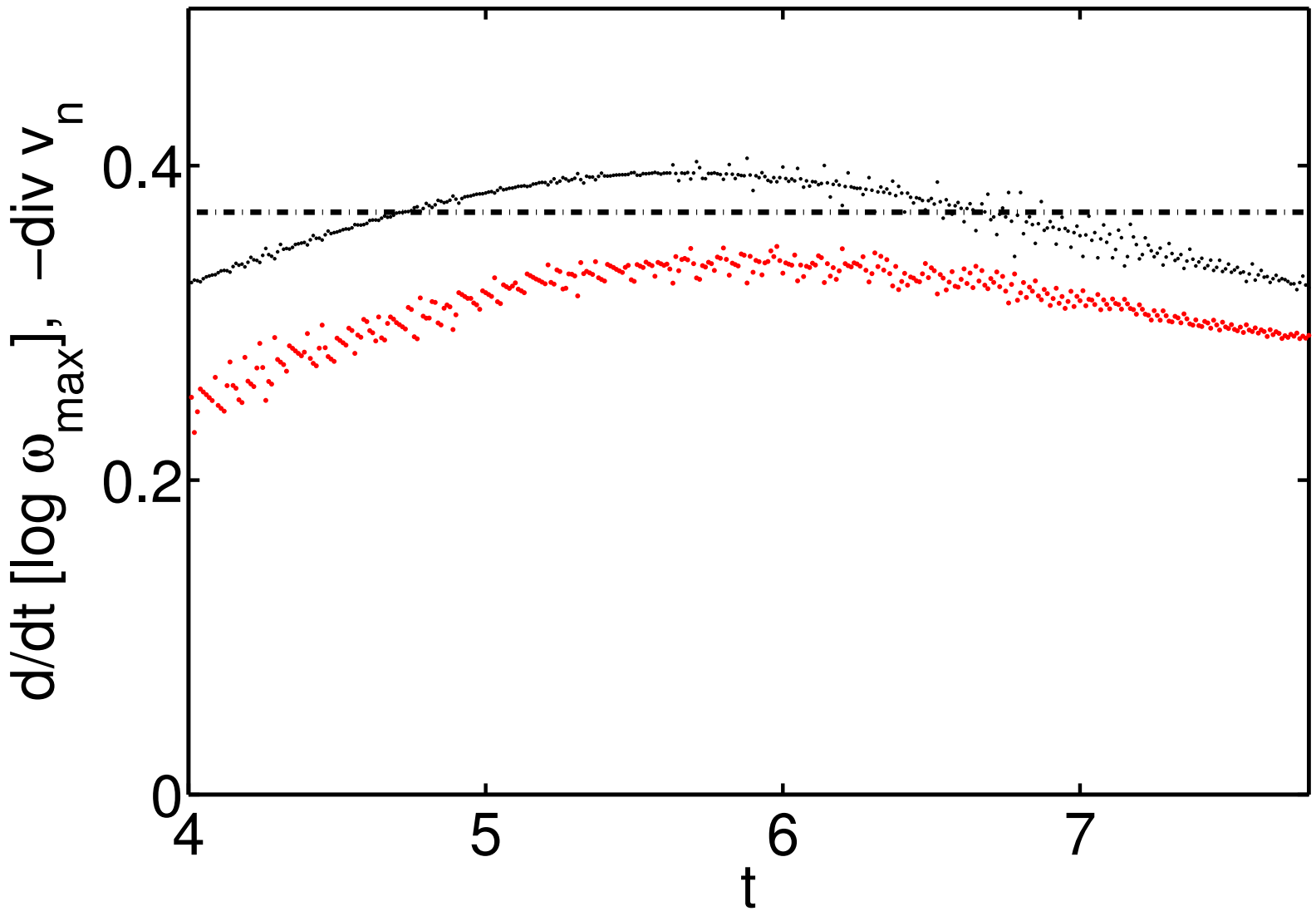

Comparison of $d \log \omega_{max}/dt$ and $-\mathrm{div}\, \mathbf{v_n}$.

Numerical experiment: compressibility

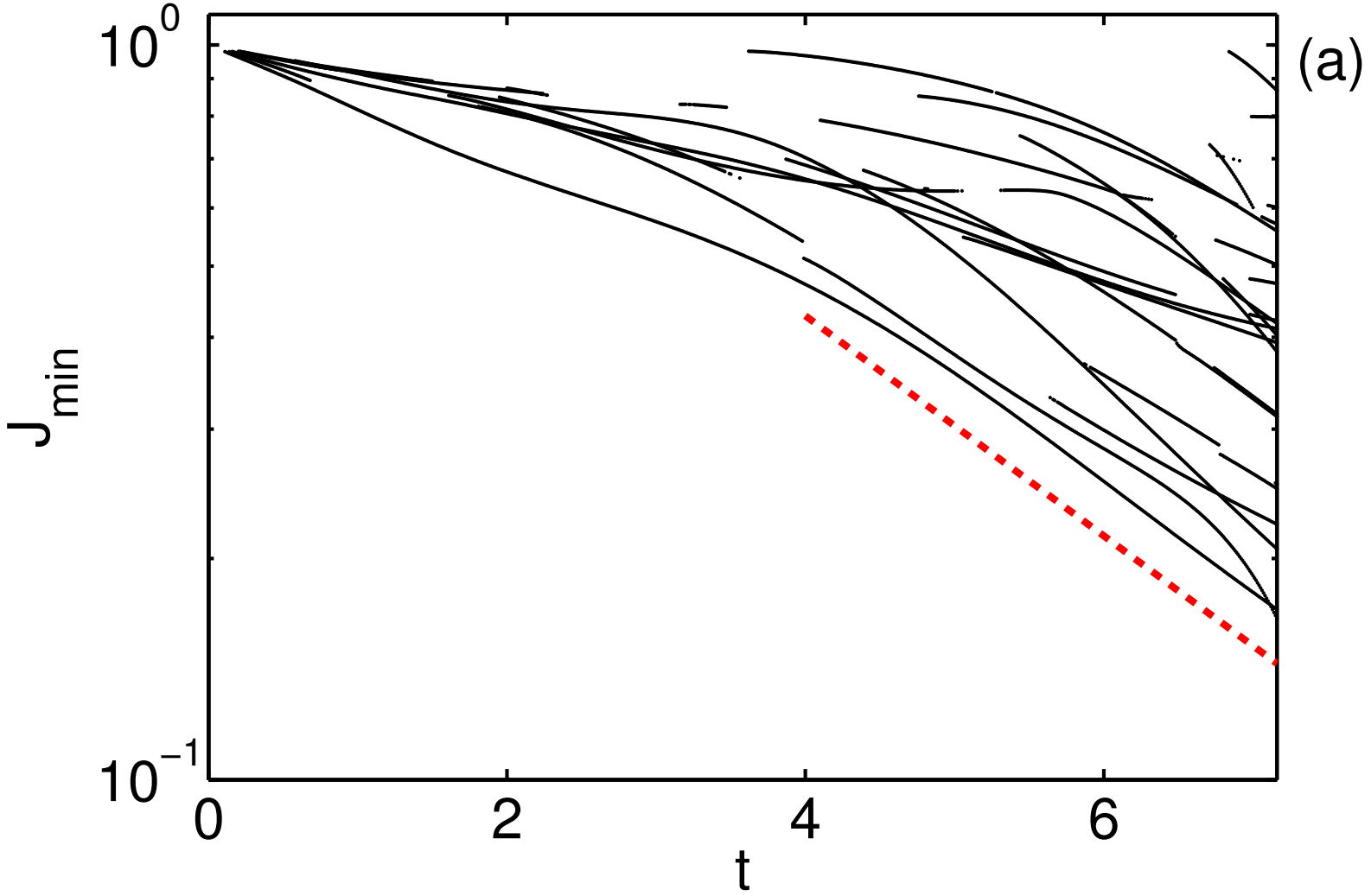

Decreasing of the Jacobian (VLR scheme)

Numerical experiment: compressibility

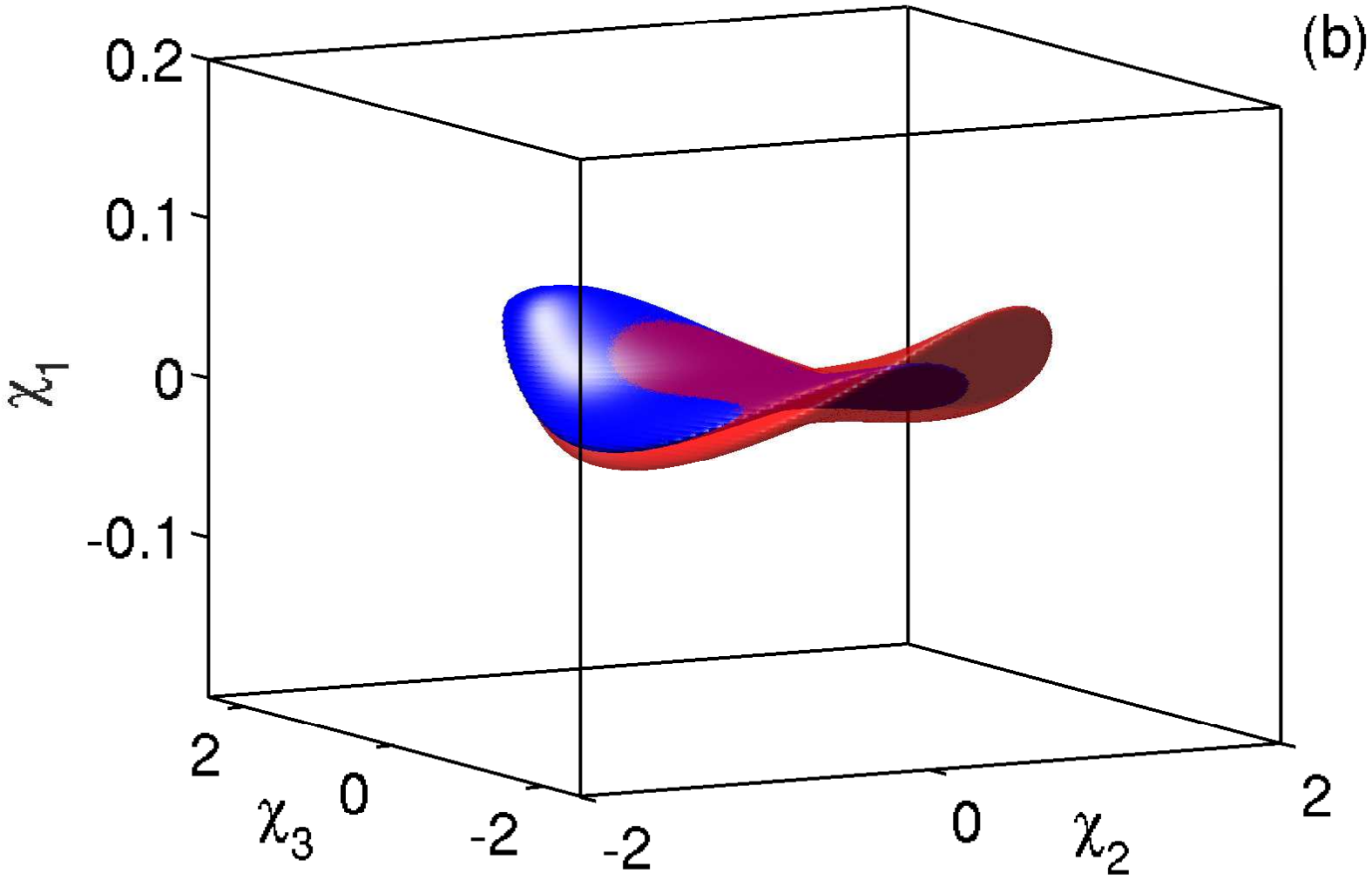

Iso-surfaces for vorticity and Jacobian (main pancake).

Numerical experiment: compressibility

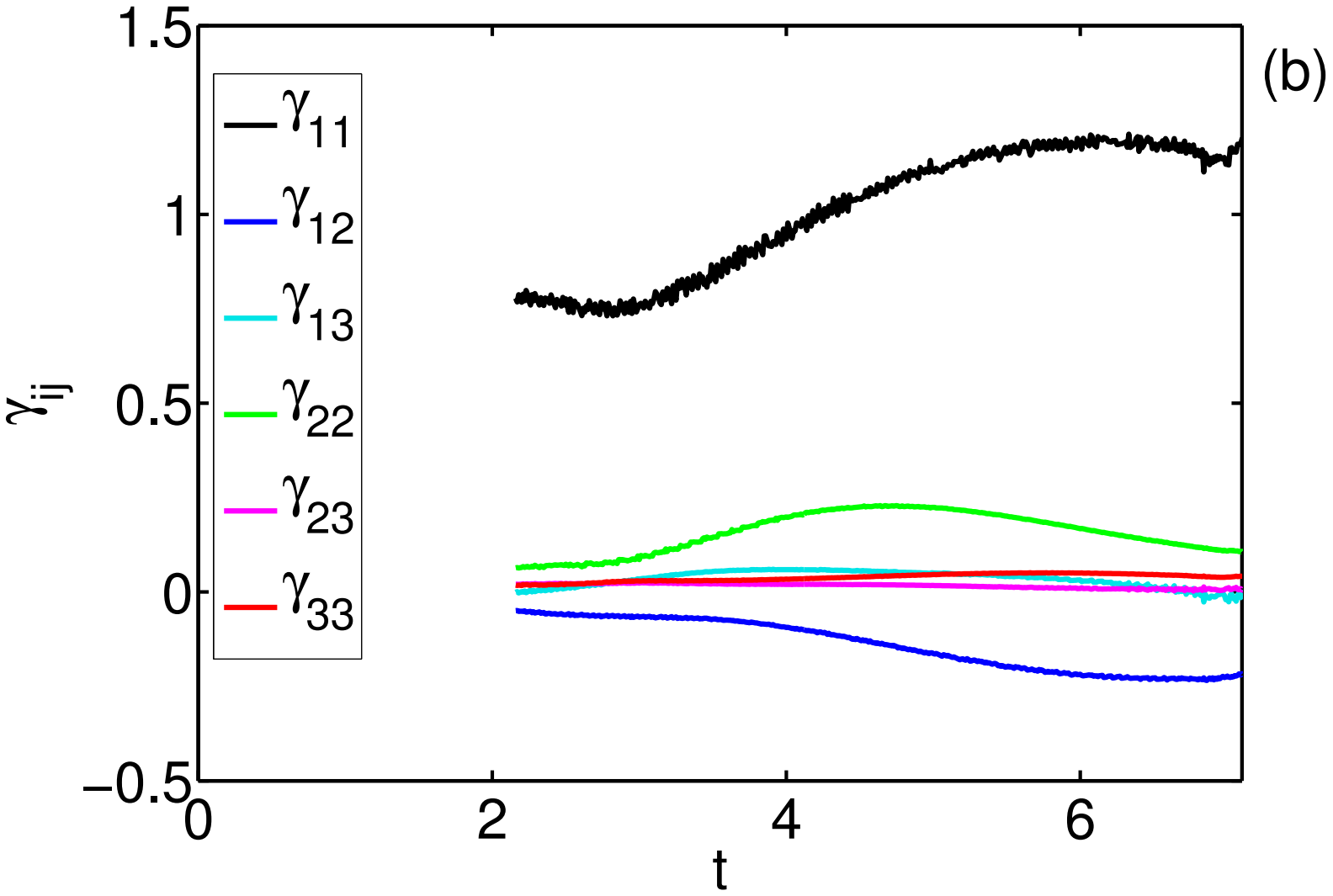

Behavior of γ_{ij} with time.

Numerical experiment

Evolution of local vorticity maximums (logarithmic vertical scale). Green line shows the global maximum, dashed red line indicates the slope $\propto e^{t/T_\omega}$ with $T_\omega = 2$.

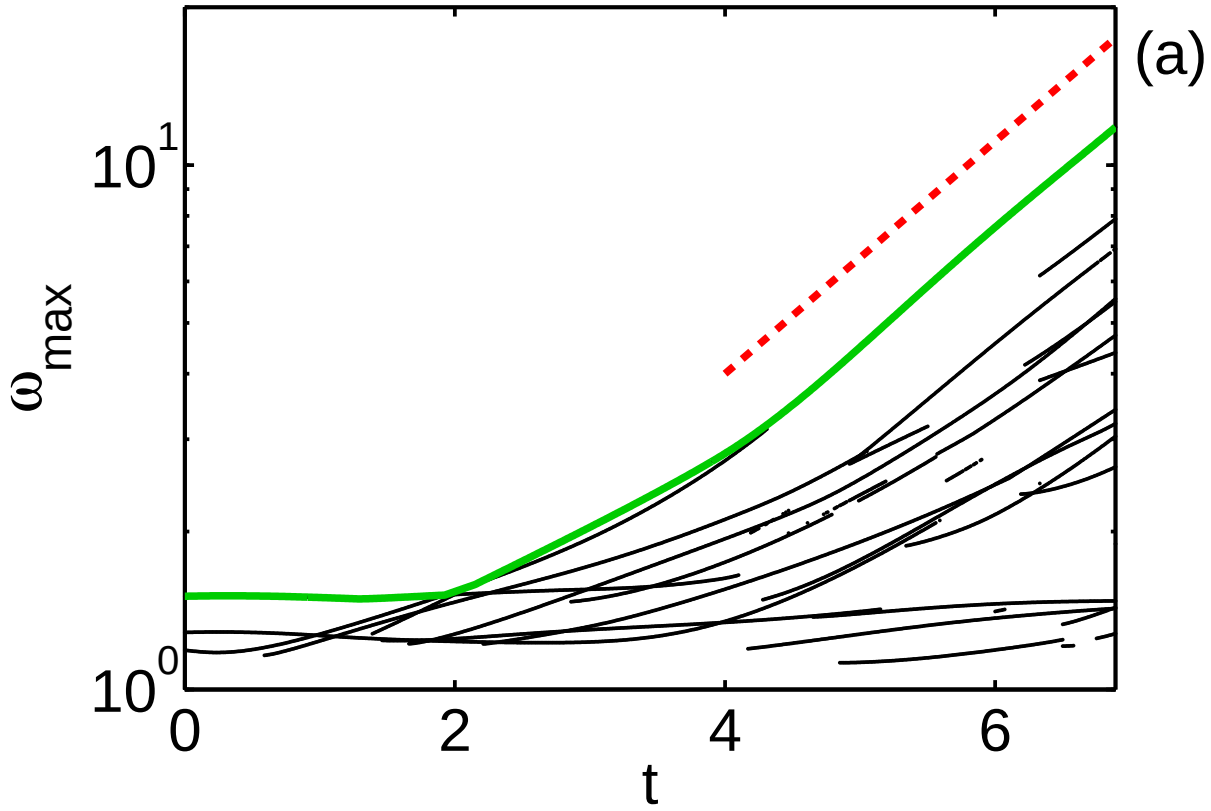

Numerical experiment

Evolution of characteristic spatial scales ℓ_1 (black), ℓ_2 (blue) and ℓ_3 (red) for the global vorticity maximum. Dashed red line indicates the slope $\propto e^{-t/T_\ell}$ with $T_\ell = 1.4$.

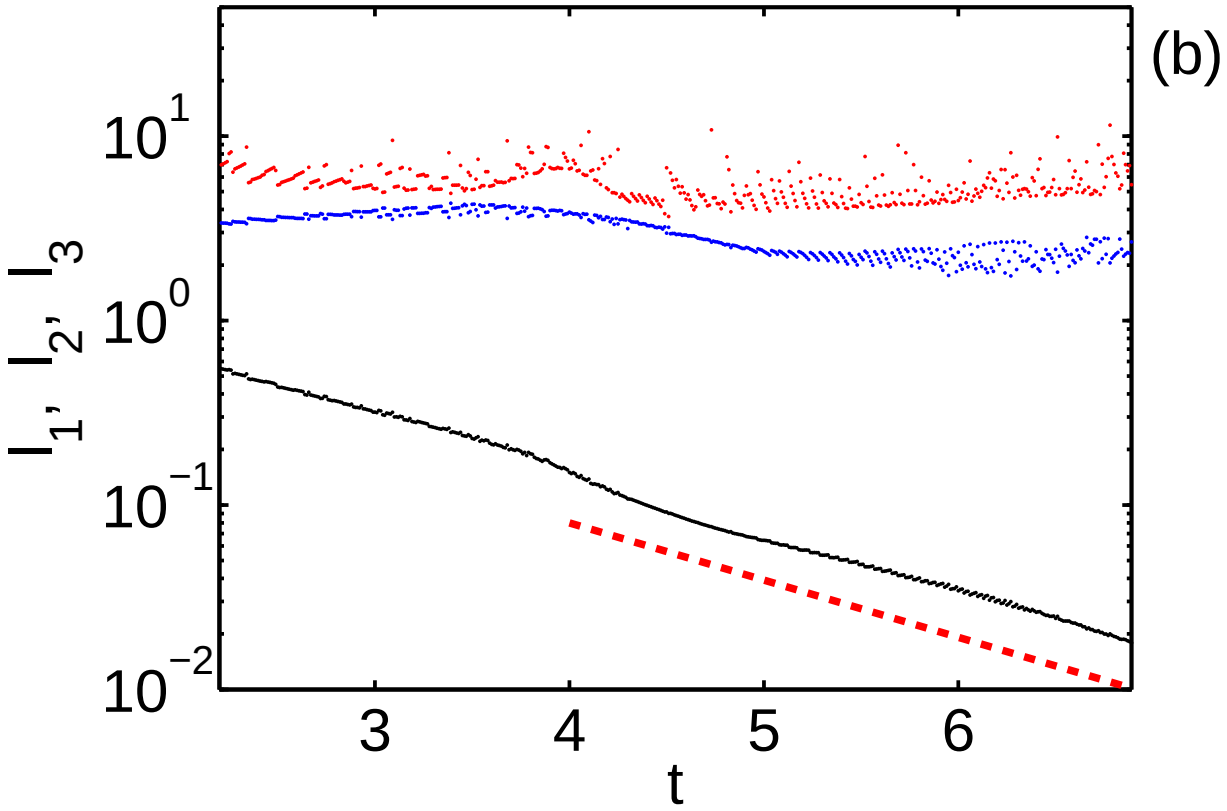

Numerical experiments

Vorticity local maximums$\omega_{\max}(t)$ vs. lengths $\ell_1(t)$ during the evolution of the pancake structures. Green line shows the global maximum, red circles mark local maximums at the final time. Dashed red line indicates the power-law $\omega_{\max} \propto \ell_1^{-2/3}$.

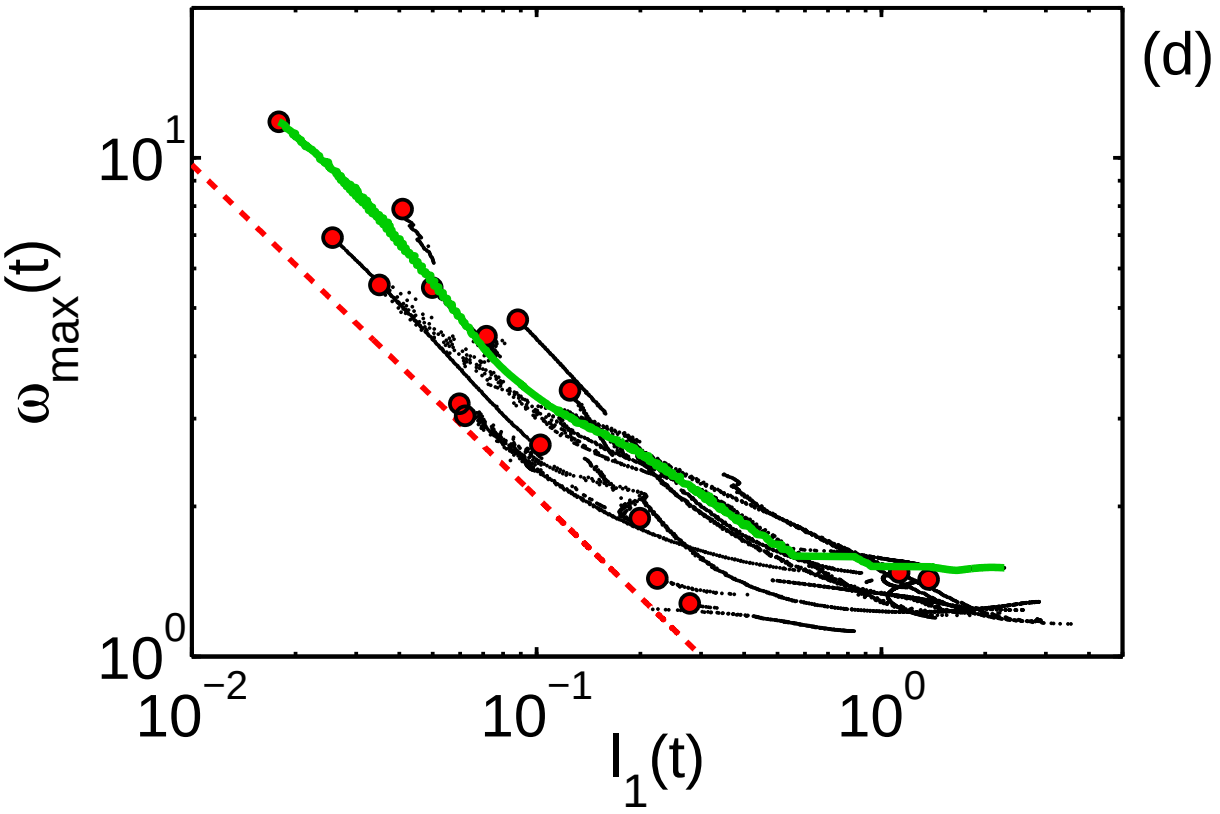

Numerical experiments

Components of the vorticity vector $\omega = (\omega_1, \omega_2, \omega_3)$ as functions of a_1 perpendicular to the pancake, at the final time.

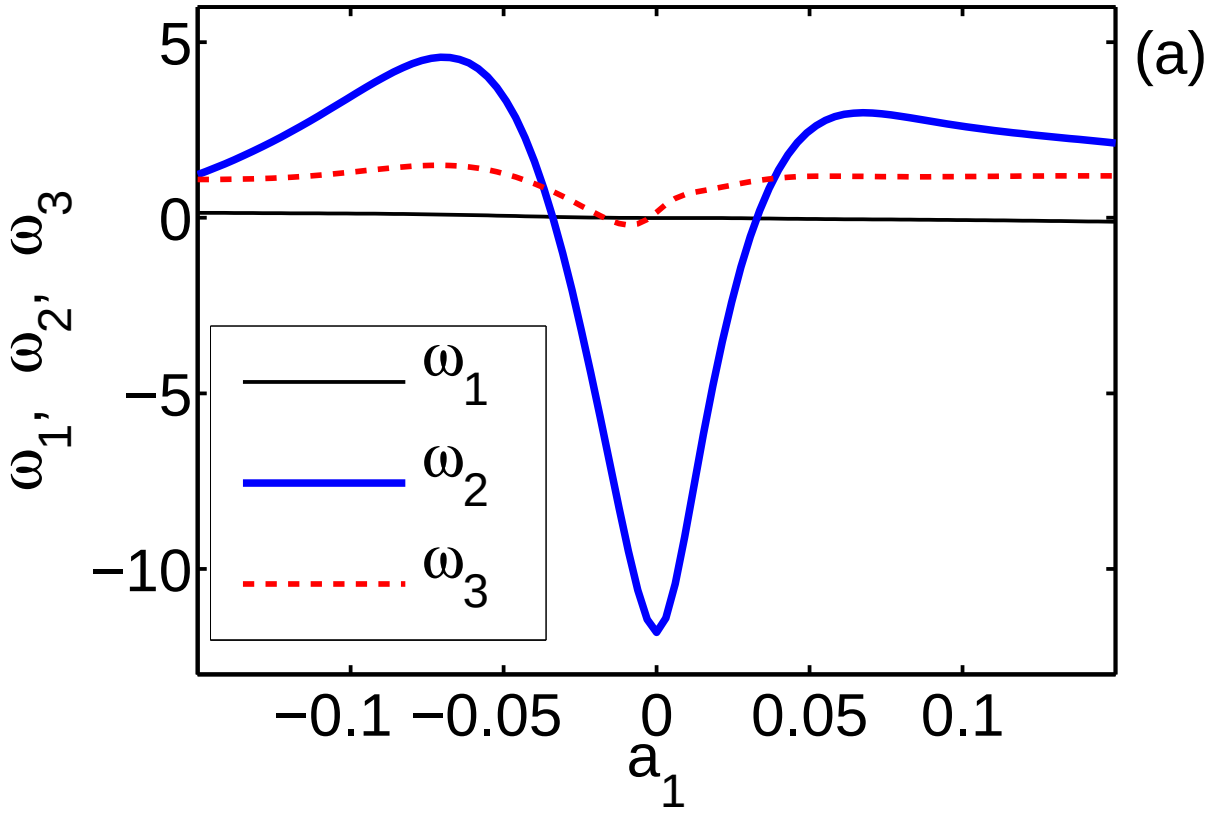

Numerical experiment

Vorticity component $\omega_2/\omega_{\max}$ vs. coordinate a_1/ℓ_1 at different times, demonstrating the self-similarity from $\ell_1(5) = 0.064$ to $\ell_1(6.89) = 0.018$.

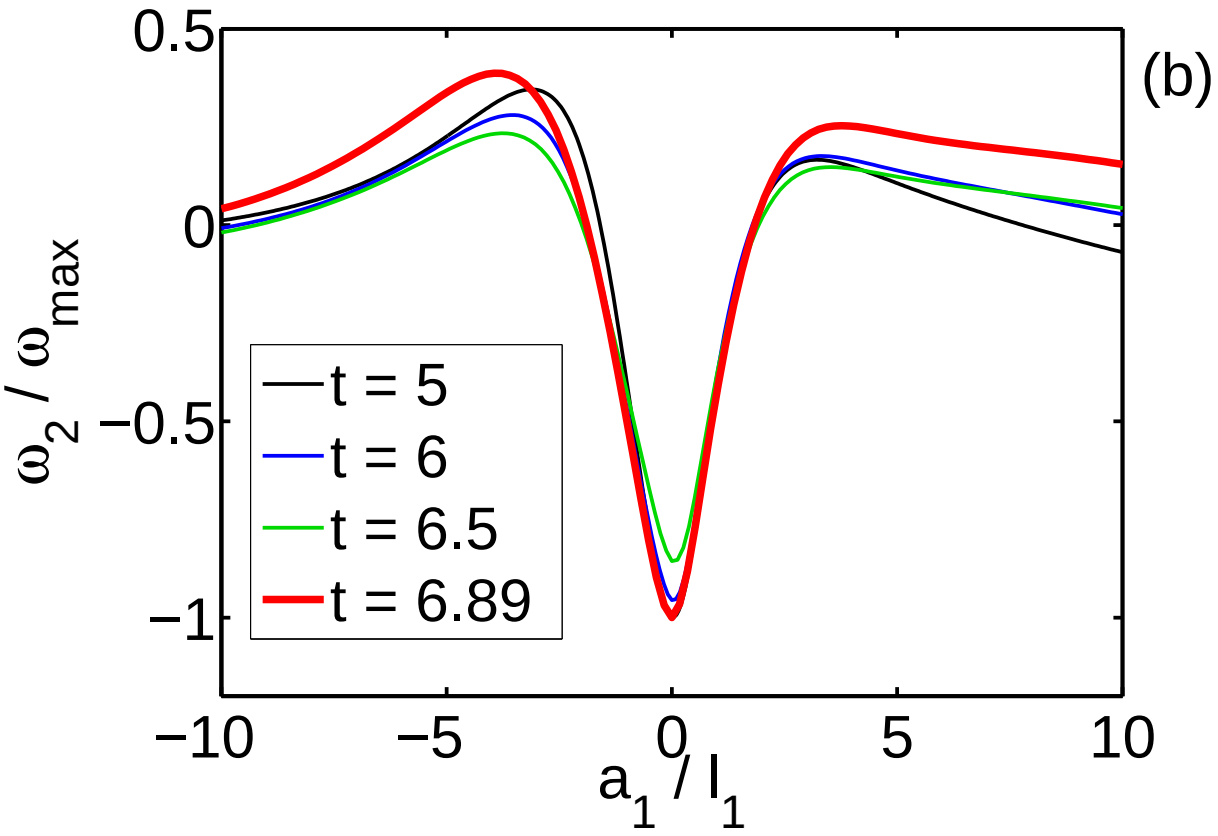

Numerical experiment

Energy spectrum at different times demonstrating the Kolmogorov power-law.

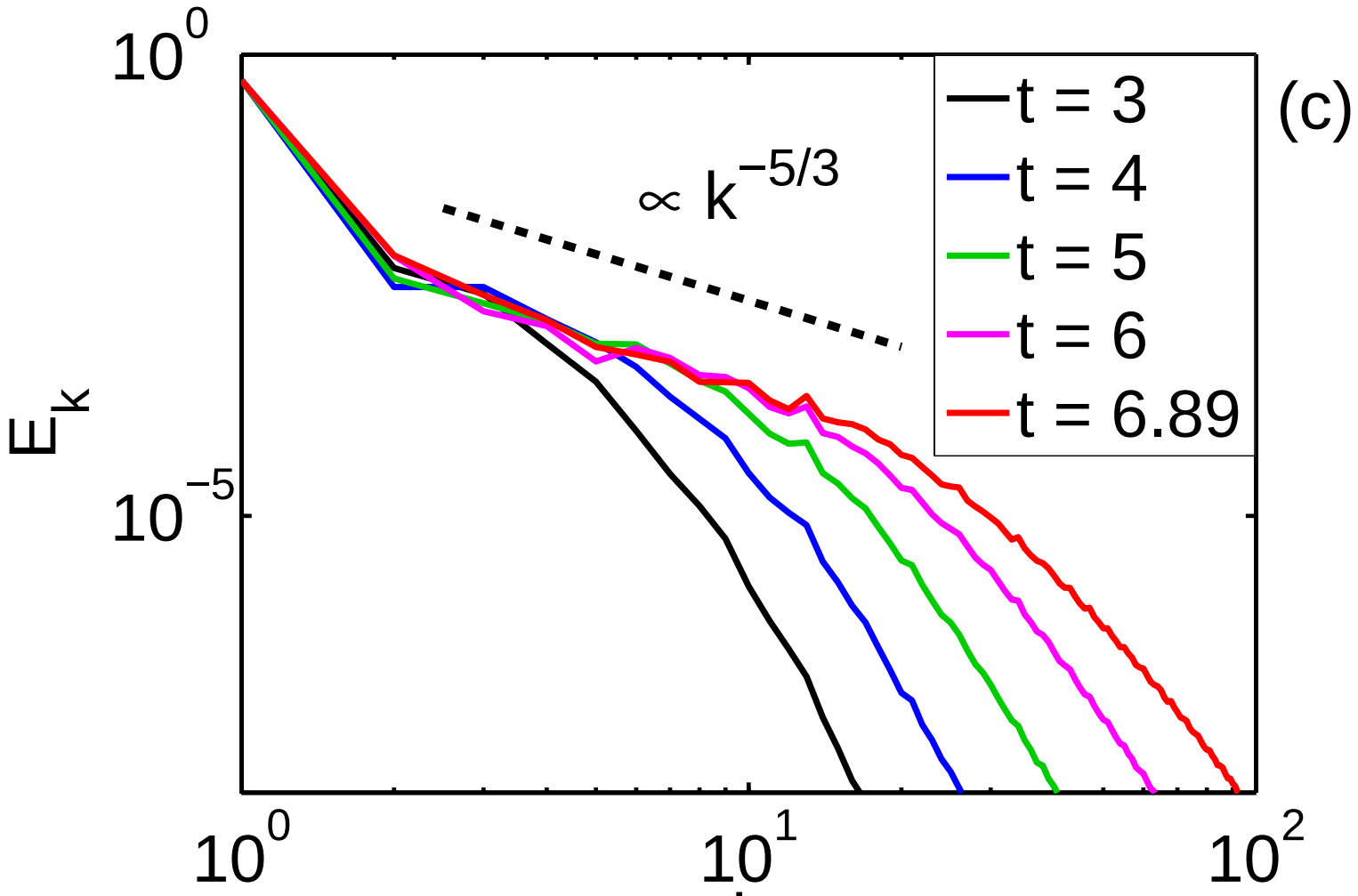

Numerical experiment: spectrum

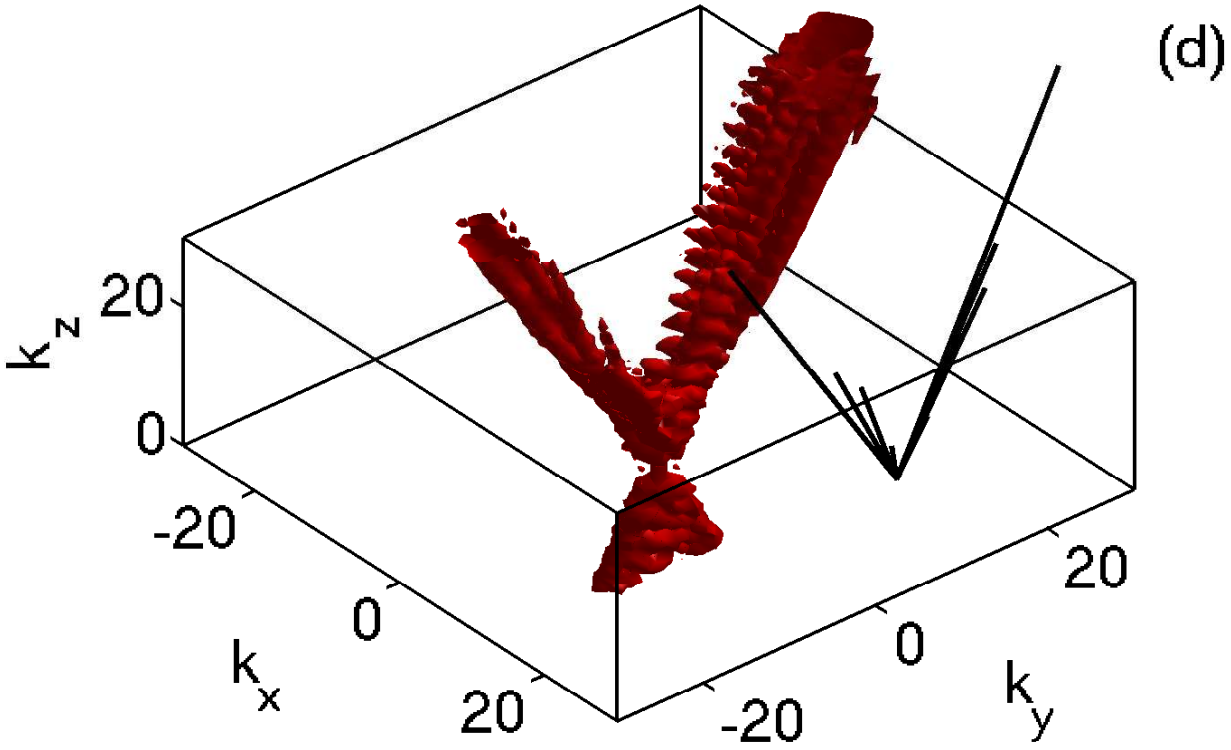

JETS: Isosurface $|\tilde{\omega}(\mathbf{k})| = 0.2$ of the normalized vorticity field in $\mathbf{k}$- space at the final time. Solid lines show maximal $\mathbf{k}$-vectors for all jets (normalized by $1/\ell_1$).

Conclusion

In this talk, based on both VLR and direct numerical integration of 3D Euler, we show:

- At the stage of turbulence arising the spectrum is very far from isotropic (in the inertial interval).
- The main contribution in the spectrum in 3D is connected with appearance of coherent structures of the pancake type which in the turbulent spectrum are responsible for jets with growing in time anisotropy. (First time such structures were observed by M. Brachet, et.al. (1992).)
- The maximal pancake vorticity and its width ℓ are connected by means of the Kolmogorov type relation:

$$\omega_{max} \sim \ell^{-2/3}.$$

Conclusion

- Appearance of the pancake structures is a consequence of compressibility of the vorticity lines as it follows from the vortex line representation (K. & Ruban, 1998, K. 2002). These structures develop in time exponentially.
- Increasing with time number of such structures leads to formation of the Kolmogorov energy spectrum observed numerically in a fully inviscid flow, with no tendency towards finite-time blowup.

References

1. E.A. Kuznetsov, V.P. Ruban, *Hamiltonian dynamics of vortex lines for systems of the hydrodynamic type*, JETP Letters, **67**, 1076-1081 (1998); *Hamiltonian dynamics of vortex and magnetic lines in the hydrodynamic type models*, Phys. Rev E, **61**, 831-841 (2000).
2. E.A. Kuznetsov,*Vortex line representation for flows of ideal and viscous fluids* , JETP Letters, **76**, 346-350 (2002); physics/0209047.
3. D.S. Agafontsev, E.A. Kuznetsov and A.A. Mailybaev, *Development of high vorticity structures in incompressible 3D Euler equations*, Physics of Fluids **27**, 085102 (2015).

References

4. D.S. Agafontsev, E.A. Kuznetsov and A.A. Mailybaev, *Development of high vorticity structures in incompressible 3D Euler equations: influence of initial conditions* JETP Letters **104**, 685Ű689 (2016).

5. D.S. Agafontsev, E.A. Kuznetsov and A.A. Mailybaev, *Asymptotic solution for high vorticity regions in incompressible 3D Euler equations*, J. Fluid Mech. **813**, R1 (1-10) (2017).

Thanks

THANKS FOR YOUR ATTENTION

THANKS TO MY CO-AUTHORS - PARTICIPANTS of THIS CONFERENCE

1. V. Zakharov
2. A. Mikhailov
3. G. Falkovich
4. S.Turitsyn
5. V. Mezentsev
6. J. Rasmussen
7. A. Newell
8. A. Dyachenko
9. V. Steinberg
10. V. Drachev

THANKS TO MY CO-AUTHORS - PARTICIPANTS of THIS CONFERENCE

11 I. Gabitov

12 P. Lushnikov

13 V. Ruban

14 F. Dias

15 V. Krasnoselskikh

16 D. Agafontsev

17 N. Erokhin

18 N. Zubarev

19 S. Minaev